Observation of a possible charge-density-wave transition in cubic $Ce_3Co_4Sn_{13}$

C. S. Lue,[1,*] H. F. Liu,[1] S.-L. Hsu,[2] M. W. Chu,[2] H. Y. Liao,[3] and Y. K. Kuo[3,†]
[1]*Department of Physics, National Cheng Kung University, Tainan 70101, Taiwan*
[2]*Center for Condensed Matter Sciences, National Taiwan University, Taipei 10601, Taiwan*
[3]*Department of Physics, National Dong Hwa University, Hualien 97401, Taiwan*
(Received 22 March 2012; published 11 May 2012)

We report an observation of a first-order phase transition in $Ce_3Co_4Sn_{13}$ by means of the specific heat, electrical resistivity, Seebeck coefficient, and thermal conductivity, as well as ^{59}Co nuclear magnetic resonance (NMR) measurements. The phase transition has been evidenced by marked features near $T_o \simeq 155$ K in all measured physical quantities except for magnetic susceptibility. This excludes a magnetic origin for the observed phase transition. In addition, x-ray diffraction results below and above T_o confirm the absence of a structural change, suggesting that the peculiar phase transition is possibly related to an electronic origin and/or electron-lattice coupling such as the formation of a charge density wave (CDW). As a matter of fact, the disappearance of the double-peak feature of ^{59}Co NMR central lines below T_o can be realized as the spatial modulation of the electric field gradient due to incommensurate CDW superlattices. Also, a distinct peak found in the spin-lattice relaxation rate near T_o manifests a phase transition and its feature can be accounted for by the thermally driven normal modes of the CDW. From the NMR analyses, we obtained a consistent picture that the change of electronic structures below T_o is mainly due to the weakening of *p-d* hybridization. Such an effect could result in possible electron-lattice instability and, thus, the formation of a CDW state in $Ce_3Co_4Sn_{13}$.

DOI: 10.1103/PhysRevB.85.205120 PACS number(s): 71.20.Eh, 71.45.Lr, 76.60.−k

I. INTRODUCTION

The intriguing charge-density-wave (CDW) phase transitions continue to attract attention in the field of solid-state physics. Such transitions usually take place in compounds with low-dimensional characters in their crystal structures, due to the instability at low temperatures against a periodic lattice distortion.[1,2] On this basis, CDW transitions are rare in three-dimensional (3D) crystal structures, and only a few 3D systems, such as CuV_2S_4, $LaAgSb_2$, $Lu_5Ir_4Si_{10}$, $Lu_2Ir_3Si_5$, and $SmNiC_2$, have been reported to possess CDW characteristics.[3–16] Associated with the CDW transitions, the electronic and thermal quantities exhibit anomalous behavior in the vicinity of the transition temperatures of these materials. Further, directly microscopic evidence for CDW formations have been confirmed from the appearance of superlattice reflections by x-ray diffraction (XRD) measurements.[3,6,10,15,17]

Recently, Thomas *et al*. noted an anomalous feature in the electrical resistivity of the ternary stannide $Ce_3Co_4Sn_{13}$ near 160 K and identified the observation as a consequence of an intrinsic phase transition.[18] From XRD measurements below and above 160 K showing the absence of a structural change in this material, the speculated structural phase transition associated with the peculiar behavior was thus ruled out.[18] Also, the transition is not likely driven by magnetic ordering because the magnetic susceptibility exhibits no appreciable anomaly around this temperature.[19] Hence, the observed phase transition should be related to an electronic origin and/or electron-lattice coupling such as the formation of a CDW driven by Fermi surface (FS) nesting due to electronic instability.

The titled compound of $Ce_3Co_4Sn_{13}$ crystallizes in a cubic $Yb_3Rh_4Sn_{13}$–type structure (space group $Pm\bar{3}n$). Within this crystal structure, the cerium and cobalt atoms occupy the 6*d* and 8*e* sites (in Wyckoff notations), respectively. Two nonequivalent crystallographic tin atoms, termed Sn(1) and Sn(2), reside at the 2*a* and 24*k* sites, respectively. The bonding length of Co-Sn(2) is the shortest among the nearest-neighbor atomic distances in $Ce_3Co_4Sn_{13}$. It is thus natural to expect a non-negligible *p-d* hybridization between the Sn(2) 5*p* and the Co 3*d* states of this compound. Such an expectation is consistent with the result of the band structure calculation, indicating a high charge density between Co and Sn(2) atoms.[20] In these respects, an examination of the possible change of electronic features, especially of the interaction between Co and Sn(2) atoms, would be essential to elucidate the intriguing phase transition in $Ce_3Co_4Sn_{13}$.

In this investigation, we performed a detailed study by means of the specific heat (C_P), electrical resistivity (ρ), Seebeck coefficient (S), and thermal conductivity (κ), as well as nuclear magnetic resonance (NMR) measurements, to shed light on the nature of the phase transition in $Ce_3Co_4Sn_{13}$. A first-order phase transition at $T_o \simeq 155$ K was discerned in the temperature dependences of the bulk properties. The NMR characteristics further provide microscopic evidence for a reduction in the Co 3*d* and Sn(2) 5*p* electronic states below the transition temperature. We associated these electronic changes with the Sn(2) atoms shifting off the original coordinates defined at room temperature. The observed phase transition behavior is similar to a CDW ordering in many aspects, presumably interpreted as electron-lattice instability due to the weakness of the *p-d* hybridization below T_o.

II. EXPERIMENTAL DETAILS

Polycrystalline $Ce_3Co_4Sn_{13}$ was prepared by a vacuum arc-melting technique. Briefly, a mixture of 99.9% Ce, 99.95% Co, and 99.99% Sn elemental metals at a stoichiometric ratio was placed in a water-cooled copper hearth and then melted several times in an argon flow arc melter. The weight loss during melting is less than 0.5%. To promote homogeneity, the as-cast sample was annealed in a vacuum-sealed quartz

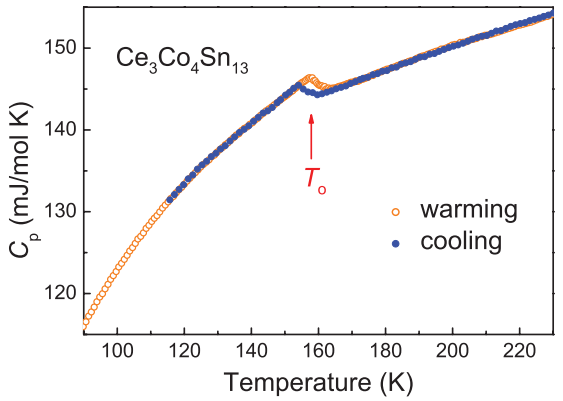

FIG. 1. (Color online) Temperature variation of the specific heat C_P for $Ce_3Co_4Sn_{13}$. The presence of thermal hysteresis near T_o indicates the first-order nature of this phase transition.

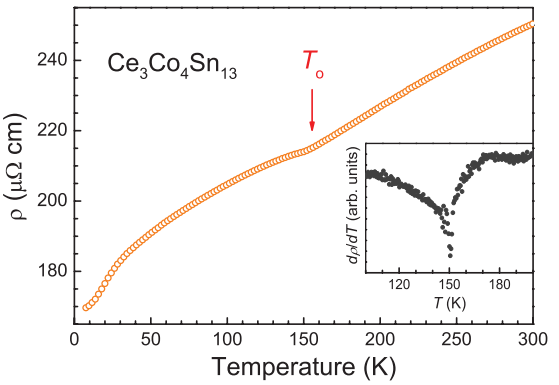

FIG. 2. (Color online) Electrical resistivity as a function of temperature for $Ce_3Co_4Sn_{13}$. Inset: Plot of $d\rho/dT$ vs T, showing a dip in the vicinity of T_o.

tube at 800° C for 3 days, followed by furnace cooling. A room-temperature XRD measurement taken with CuK_α radiation on the powdered specimen was identified within the expected cubic $Yb_3Rh_4Sn_{13}$ phase and a lattice constant $a = 9.601$ Å was determined for our $Ce_3Co_4Sn_{13}$ sample. From the NMR central transition lines, as described later, the presence of a sharp double-peak feature indicates that this material is well ordered, as the disorder effect usually broadens the NMR spectrum due to hyperfine field inhomogeneity. In addition, we carried out a low-temperature XRD experiment but found no indication of structural change compared to the room-temperature result. This is consistent with the previous observation,[18] ruling out the possibility of any structural phase transition in $Ce_3Co_4Sn_{13}$.

A. Bulk properties

Specific heat measurement was performed with a high-resolution ac calorimeter, using chopped light as the heat source. Further details about the experimental techniques for these measurements can be found elsewhere.[11] The temperature-dependent specific heat of $Ce_3Co_4Sn_{13}$ is illustrated in Fig. 1. A distinctive peak in C_p demonstrates the appearance of a phase transition at $T_o \simeq 155$ K. This observation confirms that the phase transition is an intrinsic property of $Ce_3Co_4Sn_{13}$ rather than a consequence arising from impurity phases. Also, the presence of thermal hysteresis indicates the first-order nature of this transition. As mentioned, this phase transition cannot be accounted for by either structural or magnetic origins based on the XRD and magnetic susceptibility measurements.[18,19]

Data on electrical resistivity were obtained using a standard four-point probe method. The observed temperature dependence of the electrical resistivity of $Ce_3Co_4Sn_{13}$ is displayed in Fig. 2. With decreasing temperature, ρ exhibits a metallic behavior with a broad hump appearing below T_o. Such an anomalous signature becomes clear in the $d\rho/dT$ vs T plot shown in the inset in Fig. 2. It should be noted that the temperature dependence of the electrical resistivity below T_o is different from that in the single crystal prepared by Thomas *et al.*, which shows a kink at around 160 K and then an upturn with further cooling.[18] Such semiconducting behavior suggests a small gap opening associated with this phase transition. The gap size would not be appreciable according to the weak temperature dependence of the electrical resistivity in a single crystal. In this case, the corresponding electronic band edges near the Fermi level (E_F) would be very sharp. It is commonly true that the sharp band features will be rounded in polycrystalline materials. This would cause an overlap between band edges, leading to the disappearance of the semiconducting behavior as observed in our sample. This effect might explain the discrepancy between single crystals and polycrystals of $Ce_3Co_4Sn_{13}$ in the temperature dependence of electrical resistivity below T_o. However, the characteristics of the phase transition should not change dramatically with measurement of a polycrystalline sample.

Seebeck coefficient and thermal conductivity experiments were performed simultaneously in a closed-cycle refrigerator using a heat-pulse technique. It is known that the Seebeck coefficient is a sensitive probe for the phenomenon associated with density-of-states (DOS) changes around the Fermi level, such as CDW ordering and crystallographic transition/distortion.[11,13] A plot of the measured Seebeck coefficient as a function of temperature is shown in Fig. 3. Upon cooling, S decreases quasilinearly with temperature, a typical feature for metals. The sign of S is positive, signifying that hole-type carriers dominate thermoelectric transport for

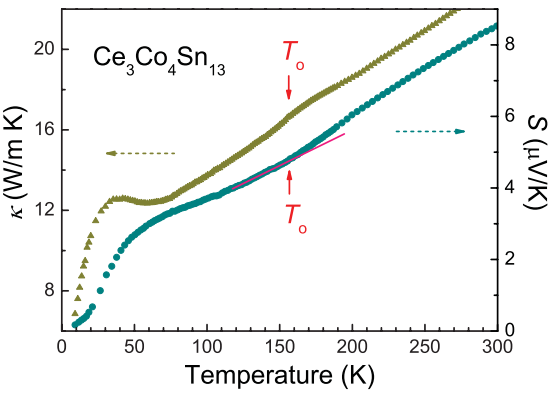

FIG. 3. (Color online) Temperature dependences of the Seebeck coefficient $S(T)$ and the total thermal conductivity $\kappa(T)$ for $Ce_3Co_4Sn_{13}$. The straight line in $S(T)$ near T_o is a guide for the eye.

$Ce_3Co_4Sn_{13}$. Below T_o, a distinct change in the slope has been noted (see the solid line in Fig. 3), pointing out the electronic origin of this transition. The T dependence of the total thermal conductivity $\kappa(T)$ for $Ce_3Co_4Sn_{13}$ is also shown in Fig 3. At low temperatures, $\kappa(T)$ develops a broad peak at around 40 K due to the reduced thermal scattering of heat-carrying phonons. In the vicinity of T_o, a small hump in $\kappa(T)$, indicated by the arrow, was observed. Therefore, the weak signatures consistently discerned in the temperature dependences of ρ, S, and κ around T_o suggest a small FS modification accompanied by the phase transition.

B. Nuclear magnetic resonance

NMR measurement is known as a local probe, providing intrinsic information on the structural and electronic characteristics of the studied material. In this investigation, NMR measurements were carried out using a Varian 300 spectrometer, with a constant field of 7.082 T. A home-built probe was employed for both room-temperature and low-temperature experiments. To avoid the skin depth problem of the radio-frequency transmission power, a powder sample was used. The specimen was put in a plastic vial that showed no observable ^{59}Co NMR signal.[21] The Knight shift here was referred to the ^{59}Co resonance frequency of 1 M aqueous $K_3Co(CN)_6$.

Since ^{59}Co NMR resonance is quadrupolar broadened, the wide-line spectrum was mapped out by integrating the spin-echo signal of various excitations. For $Ce_3Co_4Sn_{13}$, there is a single Co site, leading to a one-site NMR spectrum. Due to electric quadrupole coupling, the ^{59}Co NMR spectrum ($I = \frac{7}{2}$) consists of seven transition lines. For a powder sample, as in our experiment, these lines exhibit a typical powder pattern, with distinctive satellite lines corresponding to the quadrupole parameter. In Fig. 4, we present two fully resolved powder patterns taken at 77 and 297 K. Each quadrupole frequency ν_Q can be determined directly from the satellite lines because the first-order quadrupole shift is the major effect shaping these lines. On this basis, we obtained $\nu_Q = 0.92 \pm 0.02$ MHz for 77 K and $\nu_Q = 1.16 \pm 0.02$ MHz

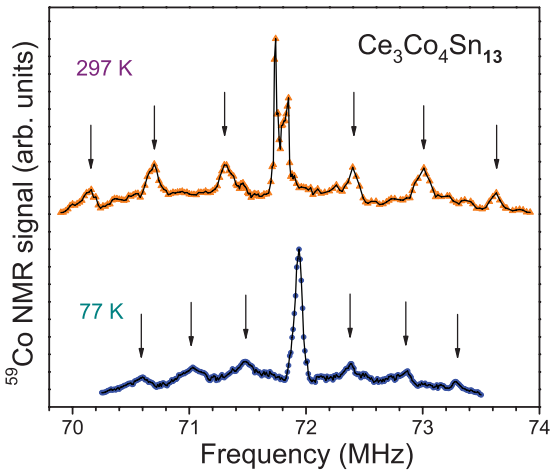

FIG. 4. (Color online) Fully resolved powder patterns for $Ce_3Co_4Sn_{13}$ measured at 297 and 77 K, respectively. For each temperature, satellite transitions are indicated by arrows.

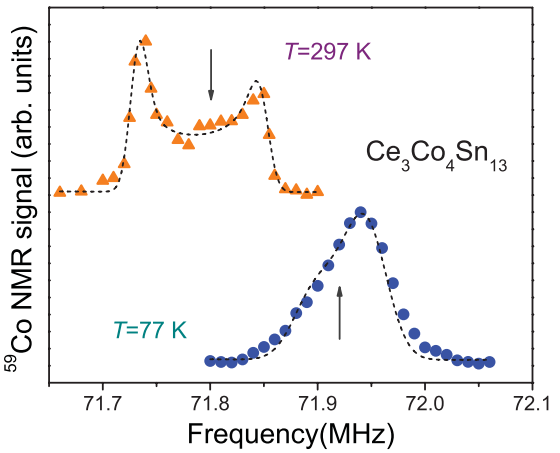

FIG. 5. (Color online) ^{59}Co NMR central transition spectra of $Ce_3Co_4Sn_{13}$ measured at 297 and 77 K, respectively. Each dashed curve is the simulated result described in the text. Each arrow indicates the position of the isotropic Knight shift (K_{iso}).

for 297 K, respectively. Here $\nu_Q = 3eQV_{zz}/2I(2I-1)h$ is defined by the nuclear quadrupole moment Q and the largest principal axis component of the electric field gradient (Za) tensor V_{zz}. The EFG sensed by the Co site of $Ce_3Co_4Sn_{13}$ is mainly due to the $5p$ electrons of the surrounding Sn(2) atoms. The apparent reduction in ν_Q below T_o reflects the fact that the local EFG becomes smaller across the phase transition. Such an observation can be associated with the decrease in the average charge density of the Sn(2) $5p$ electrons near the Fermi level. Consequently, it could weaken the hybridization between Co $3d$ and Sn(2) $5p$ electrons, leading to possible electron-lattice instability at low temperatures for $Ce_3Co_4Sn_{13}$.

Central transition ($m = \frac{1}{2} \leftrightarrow -\frac{1}{2}$) line shapes for $Ce_3Co_4Sn_{13}$ measured at 297 and 77 K were displayed in Fig. 5. The room-temperature spectrum splits into two peaks because of the simultaneous presence of anisotropic Knight shift and second-order quadrupole interactions. Below T_o, the double-peak feature becomes blurred, attributed to the weaker second-order quadrupole effect and/or spatial modulation of EFG. This is also consistent with the observation that the sharpness of the satellite line edge gradually smears out at low temperatures. Such a phenomenon is mainly due to the inhomogeneity of the local EFG, which is known to broaden the satellite line. To gain more insight into the evolution of the central transition line shape across the transition, we provide several representative spectra taken above and below T_o in Fig. 6. It is important to note that the line width does not exhibit a dramatic broadening across the transition, signifying a nonmagnetic origin for this phase transition.

Due to the cubic structure of $Ce_3Co_4Sn_{13}$, the ^{59}Co quadrupole shift and the angle-dependent Knight shift are axially symmetric. The frequency shift for the central transition, $\Delta\nu$, to the second-order quadrupole interaction and the anisotropic Knight shift can be expressed as[22]

$$\frac{\Delta\nu}{\nu_o} = \frac{K_{an}}{2(1+K_{iso})}(3\cos^2\theta - 1) + \frac{15}{16}\left(\frac{\nu_Q}{\nu_o}\right)^2(1-\cos^2\theta)(1-9\cos^2\theta). \quad (1)$$

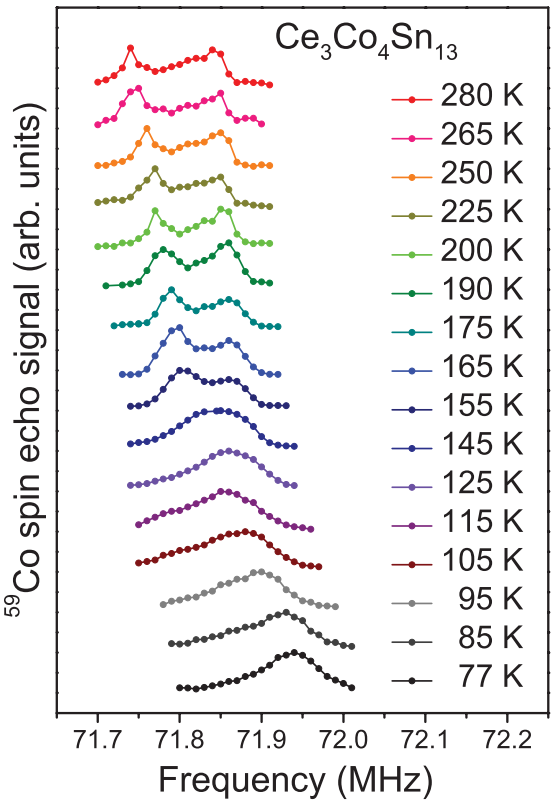

FIG. 6. (Color online) Evolution of ^{59}Co NMR central transition lines of $Ce_3Co_4Sn_{13}$ measured at various temperatures.

Here ν_o is the Larmor frequency, $K_{\rm iso}$ the isotropic Knight shift, $K_{\rm an}$ the anisotropic Knight shift, and θ the angle between the crystal symmetry axis and the external magnetic field. We performed a central line shape simulation with a proper broadening factor to reproduce the synthetic spectrum for both temperatures. To compute the line shape appropriate for a polycrystalline sample, the line shape function is, following Cohen and Reif,[23]

$$P(\nu-\nu_o)=\frac{1}{2}\left|\frac{d\nu}{d\cos\theta}\right|^{-1}. \qquad (2)$$

According to Eq. (1), the shape function possesses a step at $\nu_S=\nu_o+2a\nu_o$ and two singularities at the high frequency $\nu_H=\nu_o+b/\nu_o-a\nu_o$ and the low frequency $\nu_L=\nu_o-16b/9\nu_o-2a\nu_o/3-2a^2\nu_o^3/4b$, where $a=K_{\rm an}/2(1+K_{\rm iso})$ and $b=15\nu_Q^2/16$ for $I=7/2$. By substituting b and tuning a, the synthetic profiles were obtained. For each temperature, the best-simulated result is demonstrated as a dashed curve in Fig. 5. The simulations yield the corresponding $K_{\rm iso}=0.281\%$ and $K_{\rm an}=-0.09\%$ for 297 K and $K_{\rm iso}=0.454\%$ and $K_{\rm an}=-0.052\%$ for 77 K. In principle, the effect of spin-orbital coupling at cubic sites will cause an important contribution to $K_{\rm an}$.[24,25] Therefore, the decrease in the magnitude of $K_{\rm an}$ below $T_{\rm o}$ reflects the weakening of spin-orbital interaction. It is realistic to associate this result with the reduction in Co 3d orbital electrons at low temperatures.

The obtained temperature-dependent $K_{\rm iso}$ of $Ce_3Co_4Sn_{13}$ is displayed in Fig. 7. In general, $K_{\rm iso}$ is related to the magnetic susceptibility χ through the transferred hyperfine coupling

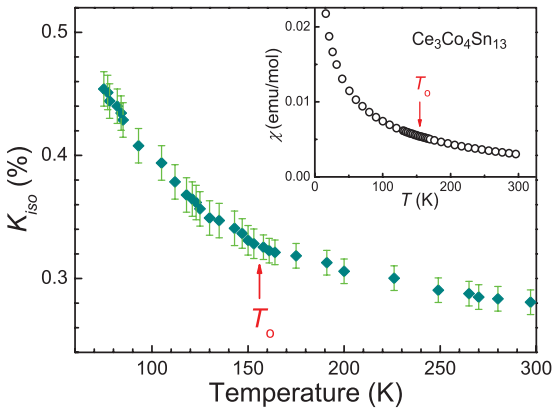

FIG. 7. (Color online) Temperature-dependent ^{59}Co NMR isotropic Knight shift for $Ce_3Co_4Sn_{13}$. Inset: Magnetic susceptibility data for $Ce_3Co_4Sn_{13}$ obtained under a constant field of 1 T.

constant $A_{\rm hf}$ as

$$K_{\rm iso}(T)=K_o+\frac{A_{\rm hf}}{N_A\mu_B}\chi(T). \qquad (3)$$

Here the temperature-independent $K_{\rm o}$ arises from the conduction electrons and the orbital shift. The constant $A_{\rm hf}$ is due to an intermixing of Co 3s and Ce 4f states for the Co site. N_A is Avogadro's constant and μ_B is the Bohr magneton. The data for χ were measured with a SQUID magnetometer (Quantum Design) under an external field of 1 T, displayed in the inset in Fig. 7. A Clogston-Jaccarino plot which shows the obtained $K_{\rm iso}$ versus χ is shown in Fig. 8. It is apparent that the linear slope changes around $T_{\rm o}$, demonstrating a significant modification in the hyperfine coupling constant across the transition. The values of $A_{\rm hf}=1.1$ kOe above $T_{\rm o}$ and $A_{\rm hf}=2.1$ kOe below $T_{\rm o}$ were extracted. The difference between the values of $A_{\rm hf}$ is associated with the change in the coupling between Ce 4f and conduction electrons. Based on the theoretical calculation,[20] the observed enhancement of the f-s coupling can be associated with the weakening of the p-d hybridization below the transition temperature of $Ce_3Co_4Sn_{13}$. Accordingly, the Ce 4f electrons occupy the antibonding states near E_F and thus have a strong mixture

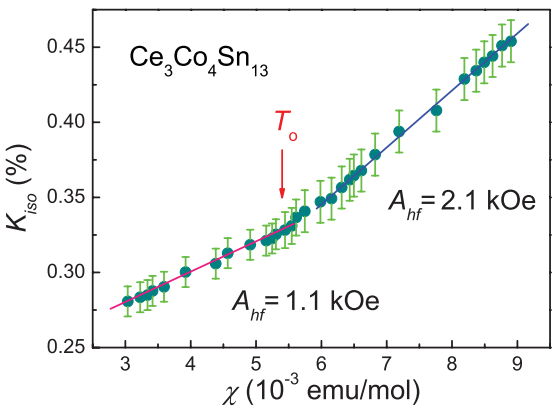

FIG. 8. (Color online) Variation of $K_{\rm iso}$ versus χ for $Ce_3Co_4Sn_{13}$. The two straight lines indicate the slope change across the phase transition.

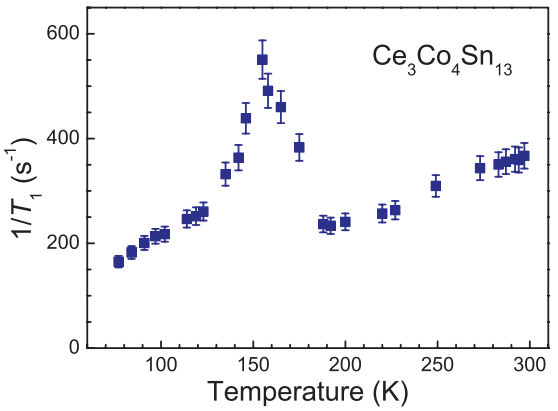

FIG. 9. (Color online) Temperature dependence of the ^{59}Co spin-lattice relaxation rate in $Ce_3Co_4Sn_{13}$.

with conduction electrons. Also, Ce 5*d* electrons make partial contributions to the total *p*-*d* hybridized states, leading to a significant interplay between the *f*-*s* interaction and the *p*-*d* hybridization for $Ce_3Co_4Sn_{13}$.[20] It should be pointed out that the relatively strong *f*-*s* coupling at low temperatures could be a key factor responsible for the nonmagnetic ground state of this compound.[26,27]

Spin-lattice relaxation rate $(1/T_1)$ measurement was carried out using the inversion recovery method. We recorded the recovery of the signal strength by integrating the ^{59}Co spin-echo signal. In this experiment, the relaxation process involves adjacent pairs of spin levels, and the corresponding spin-lattice relaxation is a multiexponential expression. For the central transition with $I = \frac{7}{2}$, the time-dependent nuclear magnetization $M(t)$ follows:

$$M(t) \propto \left(0.0286e^{-\frac{t}{T_1}} + 0.178e^{-\frac{6t}{T_1}} + 0.794e^{-\frac{15t}{T_1}}\right). \quad (4)$$

Each T_1 value was thus obtained by fitting to the multiexponential function.

The temperature variation of $1/T_1$ for $Ce_3Co_4Sn_{13}$ is illustrated in Fig. 9. While the quantitative analysis of $1/T_1$ is somewhat complicated, the presence of a peak feature in $1/T_1$ clearly manifests an intrinsic phase transition at $\simeq$155 K. Since the phase transition cannot be accounted for by the magnetic origin, the observed peak is not interpreted as the result of the rapid fluctuations of the spin dynamics arising from magnetic ordering. Rather, the likely mechanism is thermally driven normal modes of the CDW,[28] and the peak behaves quite similarly to that in the typical incommensurate CDW ordering of $NbSe_3$.[29]

III. DISCUSSION

The present investigation shows clear evidence of a first-order phase transition at around 155 K in $Ce_3Co_4Sn_{13}$ involved with the changes in electronic structures. The result of ^{59}Co NMR quadrupole splitting indicates a marked reduction in the Sn(2) 5*p* electronic density based on the weaker local EFG at low temperatures. The change in electronic states is very likely due to the slight movement and/or distortion of the Sn(2) atom from its initial position, because this site resides in the only crystallographic site showing an active spatial degree of freedom within the structure. As a consequence, the strength of the *p*-*d* hybridization decreases at low temperatures, providing an opportunity to give rise to electron-lattice instability. This could result in a nesting of FSs along a particular wave vector direction, which may facilitate CDW formation.

While the features presented here are reminiscent of those in CDW materials, the relatively weak anomalies in the vicinity of T_o imply that only a small segment of the FS is being gapped below T_o. As a matter of fact, complicated band structures in $Ce_3Co_4Sn_{13}$ have been pointed out by theoretical calculations, and some bands exhibit flat curvature regions with the characteristics for possible nesting.[20] Meanwhile, the indiscernible feature in the magnetic susceptibility around the phase transition region could be explained by the fact that the large local moment contribution from Ce^{3+} ions overwhelms the small change arising from the DOS reduction. Similar observations have been reported in the CDW systems of $Er_5Ir_4Si_{10}$ and $SmNiC_2$, also attributed to the dominance of local moments that overwhelms any changes in the Pauli paramagnetism.[30,31]

In further attempts to tackle structurally the possible existence of a CDW state, we performed powder XRD measurements down to 10 K using a synchrotron radiation source. Nevertheless, no reflections in addition to those of the parent $Pm\bar{3}n$ symmetry were observed. This result infers that the superlattice reflections could be too weak to be detected on the basis of such an averaging technique, if there is indeed a CDW state below T_o. It is worthwhile mentioning that the anomalous feature in the electrical resistivity of $Sr_3Ir_4Sn_{13}$ at around 147 K behaves quite similarly to that in the present case of $Ce_3Co_4Sn_{13}$. The signature has been associated with the nesting of FSs, which has been connected to the CDW instability based on the single-crystal XRD result.[32] Hence, the unambiguous CDW state in $Ce_3Co_4Sn_{13}$ will have to wait until the identification of superlattice reflections on a single crystal by XRD.

IV. CONCLUDING REMARKS

To summarize, $Ce_3Co_4Sn_{13}$ undergoing a first-order phase transition near 155 K has been established by bulk properties and NMR measurements. Since no corresponding anomaly was observed in the magnetic susceptibility, the transition is most likely not connected to a magnetic origin. From the low-temperature XRD result, we have confirmed that the observed anomalies are not relevant to a classical structural phase transition. In addition, the NMR analyses provide concrete evidence that the phase transition is essentially related to the strength of the *p*-*d* hybridization between the Sn(2) 5*p* and the Co 3*d* states of this compound. Upon cooling below T_o, the NMR observations indicate the relatively weak *p*-*d* hybridization, which may give rise to an electronically driven lattice distortion. Furthermore, the NMR line shapes together with the $1/T_1$ characteristics were found to be consistent with those observed in the CDW

materials. In these respects, $Ce_3Co_4Sn_{13}$ appears to be an interesting system to study the mechanism behind the possible CDW state without involving the complexities related to magnetism and superconductivity and thus deserves further investigation.

ACKNOWLEDGMENTS

This work was supported by the National Science Council of Taiwan under Grant Nos. NSC-98-2112-M-006-011-MY3 (C.S.L.) and NSC-100-2628-M-259-001-MY3 (Y.K.K.).

*Corresponding author: cslue@mail.ncku.edu.tw
†ykkuo@mail.ndhu.edu.tw

[1]H. Frohlich, Proc. R. Soc. London A **223**, 296 (1954).
[2]R. E. Peierls, in *Quantum Theory of Solids* (Oxford University Press, London, 1955), p. 108.
[3]R. M. Fleming, F. J. DiSalvo, R. J. Cava, and J. V. Waszczak, Phys. Rev. B **24**, 2850 (1981).
[4]F. J. DiSalvo and J. V. Waszczak, Phys. Rev. B **26**, 2501 (1982).
[5]K. D. Myers, S. L. Bud'ko, I. R. Fisher, Z. Islam, H. Kleinke, A. H. Lacerda, and P. C. Canfield, J. Magn. Magn. Mater. **205**, 27 (1999).
[6]C. Song, J. Park, J. Koo, K.-B. Lee, J. Y. Rhee, S. L. Bud'ko, P. C. Canfield, B. N. Harmon, and A. I. Goldman, Phys. Rev. B **68**, 035113 (2003).
[7]S. L. Bud'ko, T. A. Wiener, R. A. Ribeiro, P. C. Canfield, Y. Lee, T. Vogt, and A. H. Lacerda, Phys. Rev. B **73**, 184111 (2006).
[8]C. S. Lue, Y. F. Tao, K. M. Sivakumar, and Y. K. Kuo, J. Phys. Condens. Matter **19**, 406230 (2007).
[9]H. D. Yang, P. Klavins, and R. N. Shelton, Phys. Rev. B **43**, 7688 (1991).
[10]B. Becker, N. G. Patil, S. Ramakrishnan, A. A. Menovsky, G. J. Nieuwenhuys, J. A. Mydosh, M. Kohgi, and K. Iwasa, Phys. Rev. B **59**, 7266 (1999).
[11]Y.-K. Kuo, C. S. Lue, F. H. Hsu, H. H. Li, and H. D. Yang, Phys. Rev. B **64**, 125124 (2001).
[12]Y. Singh, D. Pal, S. Ramakrishnan, A. M. Awasthi, and S. K. Malik, Phys. Rev. B **71**, 045109 (2005).
[13]Y. K. Kuo, K. M. Sivakumar, T. H. Su, and C. S. Lue, Phys. Rev. B **74**, 045115 (2006).
[14]M. Murase, A. Tobo, H. Onodera, Y. Hirano, T. Hosaka, S. Shimomura, and N. Wakabayashi, J. Phys. Soc. Jpn. **73**, 2790 (2004).
[15]S. Shimomura, C. Hayashi, G. Asaka, N. Wakabayashi, M. Mizumaki, and H. Onodera, Phys. Rev. Lett. **102**, 076404 (2009).
[16]A. Wolfel, L. Li, S. Shimomura, H. Onodera, and S. van Smaalen, Phys. Rev. B **82**, 054120 (2010).
[17]M. H. Lee, C. H. Chen, M.-W. Chu, C. S. Lue, and Y. K. Kuo, Phys. Rev. B **83**, 155121 (2011).
[18]E. L. Thomas, H. O. Lee, A. N. Bankston, S. MaQuilon, P. Klavins, M. Moldovan, D. P. Young, Z. Fisk, and J. Y. Chan, J. Solid State Chem. **179**, 1642 (2006).
[19]C. Israel, E. M. Bittar, O. E. Aguero, R. R. Urbano, C. Rettori, I. Torriani, P. G. Pagliuso, N. O. Moreno, J. D. Thompson, M. F. Hundley, J. L. Sarrao, and H. A. Borges, Physica B **359–361**, 251 (2005).
[20]G. Zhong, X. Lei, and J. Mao, Phys. Rev. B **79**, 094424 (2009).
[21]C. S. Lue and S. C. Chen, Phys. Rev. B **79**, 125108 (2009).
[22]W. H. Jones Jr., T. P. Graham, and R. G. Barnes, Phys. Rev. **132**, 1898 (1963).
[23]M. H. Cohen and F. Reif, in *Solid State Physics*, edited by F. Seitz and D. Turnbull, Vol. 5 (Academic Press, New York, 1957), p. 311.
[24]A. Rubens, B. de Castro, and R. T. Schumacher, Phys. Rev. B **7**, 105 (1973).
[25]G. S. Tripathi, L. K. Das, P. K. Misra, and S. D. Mahanti, Phys. Rev. B **25**, 3091 (1982).
[26]A. L. Cornelius, A. D. Christianson, J. L. Lawrence, V. Fritsch, E. D. Bauer, J. L. Sarrao, J. D. Thompson, and P. G. Pagliuso, Physica B **378–380**, 113 (2006).
[27]A. D. Christianson, J. S. Gardner, H. J. Kang, J.-H. Chung, S. Bobev, J. L. Sarrao, and J. M. Lawrence, J. Magn. Magn. Mater. **310**, 266 (2007).
[28]R. Blinc, Phys. Rep. **79**, 331 (1981).
[29]B. H. Suits and C. P. Slichter, Phys. Rev. B **29**, 41 (1984).
[30]F. Galli, S. Ramakrishnan, T. Taniguchi, G. J. Nieuwenhuys, J. A. Mydosh, S. Geupel, J. Ludecke, and S. van Smaalen, Phys. Rev. Lett. **85**, 158 (2000).
[31]H. Onodera, Y. Koshikawa, M. Kosaka, M. Ohashi, H. Yamauchi, and Y. Yamaguchi, J. Magn. Magn. Mater. **182**, 161 (1998).
[32]L. E. Klintberg, S. K. Goh, P. L. Alireza, P. J. Saines, D. A. Tompsett, P. W. Logg, J. Yang, B. Chen, K. Yoshimura, and F. M. Grosche, e-print arXiv:1202.3282.